minerals

MDPI

Article

Study on the Rheological and Thixotropic Properties of Fiber-Reinforced Cemented Paste Backfill Containing Blast Furnace Slag

Xulin Zhao [1], Haijun Wang [1,2,*], Guanghua Luo [3], Kewei Dai [3], Qinghua Hu [3], Junchao Jin [2], Yang Liu [1], Baowen Liu [3], Yonggang Miao [1], Kunlei Zhu [1], Jianbo Liu [1], Hai Zhang [3], Lianhe Wu [3], Jianming Wu [3], Yueming Lu [3], Wei Wang [3] and Dingchao Lv [4]

[1] BGRIMM Technology Group, Beijing 100160, China; zhaoxulin@bgrimm.com (X.Z.); liuyang2@bgrimm.com (Y.L.); miaoyonggang@bgrimm.com (Y.M.); zhukunlei@bgrimm.com (K.Z.); liujianbo@bgrimm.com (J.L.)
[2] China Nonferrous Metal Mining (Group) Co., Ltd., Beijing 100029, China; jinjunchao2008@163.com
[3] Ganfeng Lithium Group Co., Ltd., Xinyu 338000, China; luoguanghua@ganfenglithium.com (G.L.); daikewei@ganfenglithium.com (K.D.); huqinghuacsu@163.com (Q.H.); gurk73@163.com (B.L.); zhanghai01504130@163.com (H.Z.); so51mn@163.com (L.W.); ctbwjm@126.com (J.W.); 13674863094@163.com (Y.L.); wangwei_722@163.com (W.W.)
[4] Shanxi Zijin Mining Co., Ltd., Xinzhou 034302, China; salman_zhao@126.com
* Correspondence: wnacky@163.com

Abstract: To investigate the mechanism of polypropylene fiber (PPF) on the rheological and thixotropic properties of cemented paste backfill containing mineral admixtures, the concept of water film thickness (WFT) was introduced. The packing density of the tailings-binder-PPF (TBP) system was measured in dry and wet conditions and the WFT was calculated accordingly. Additionally, the rheological parameters (yield stress, thixotropy, etc.) of the fiber-reinforced cemented paste backfill (FRCPB) were quantified. The results demonstrate that the wet packing test is a more appropriate method for measuring the packing density of the TBP system. The PPF length has a slight adverse effect on the packing density, and the packing density initially increases and then decreases with the PPF content. The reasons can be attributed to the filling effect and wedge effect of the fibers, respectively. In addition to the packing density, the thixotropy of FRCPB is also affected by the interaction of fibers. WFT is a crucial factor affecting the yield stress of FRCPB, with which it exhibits a strong linear relationship. The study identified that the optimum PPF content for enhancing the rheological and thixotropic properties of CPB is 0.2%, with a fiber length of 9 mm, balancing flowability and stability for practical application in mining backfill operations. These insights can guide the optimization of CPB mixtures, enhancing their flowability and stability during placement in mined-out spaces. By improving the fill quality and reducing the risk of blockage during backfill operations, the results offer practical benefits in increasing the safety and efficiency of underground mining activities.

Keywords: polypropylene fiber; cemented paste backfill; packing density; water film thickness; yield stress; thixotropy

Citation: Zhao, X.; Wang, H.; Luo, G.; Dai, K.; Hu, Q.; Jin, J.; Liu, Y.; Liu, B.; Miao, Y.; Zhu, K.; et al. Study on the Rheological and Thixotropic Properties of Fiber-Reinforced Cemented Paste Backfill Containing Blast Furnace Slag. *Minerals* **2024**, *14*, 964. https://doi.org/10.3390/min14100964

Academic Editors: Shiyu Zhang, Erol Yilmaz, Chen Hou and Mamadou Fall

Received: 12 August 2024
Revised: 15 September 2024
Accepted: 23 September 2024
Published: 24 September 2024

1. Introduction

Cemented paste backfill (CPB), as a green and efficient mining technology, has been widely used and studied around the world in recent years [1–4]. Compared with traditional mining methods, CPB technology has unique advantages and potential. First of all, CPB can maximize the recovery and utilization of ore resources, thereby improving the efficiency of ore mining and recovery [5–8]. In addition, CPB can reduce the risk of surface subsidence and geological disasters and effectively protect the integrity of the surface environment and ecosystem [9]. However, the traditional CPB still has some limitations in practice, such as high brittleness and low flexural and tensile strength [10,11]. Under the action of mining

disturbance, CPB is easily prone to the phenomenon of rib spalling [12]. To overcome these problems and further optimize the performance of CPB, fiber-reinforced cemented paste backfill (FRCPB) was presented. This is a method of mixing fibers with traditional CPB to form backfill materials with good toughness and flexural/tensile strength [13]. Compared with traditional CPB, FRCPB significantly improves the above shortcomings and has extremely high on-site significance.

At present, the hardened properties of FRCPB, such as uniaxial compressive strength and flexural strength, have been extensively studied. Xue et al. [14–16] and Cao et al. [17] studied the effects of fiber characteristics such as fiber type and length on the strength characteristics, failure behavior, and microstructure of FRCPB. Chen et al. [18] explored the effects of fiber content and length on the compressive behavior and microstructural properties of CPB. Sun and Fall [19] used the response surface methodology to characterize and optimize the key engineering properties of fiber-reinforced cemented tailings backfill, such as strength and elastic modulus. Cui et al. [20] studied the evolutive fracture behavior and properties of FRCPB under pure mode-I, mode-II, and mode-III loadings. Guo et al. [21] used recycled tire polymer fiber (RTPF) to replace polypropylene fiber (PPF). The results showed that with the addition of 0.6% RTPF, the strength properties of cemented tailings backfill were comparable to those of CPB containing 0.3% PPF. These studies are of great significance for understanding the hardened properties of FRCPB. However, it is worth noting that there are relatively few studies on the rheological properties of fresh FRCPB [21]. In addition, the mechanism of fibers on the rheological properties of CPB also needs to be further explored. A full understanding of the rheological properties of CPB is critical to its transportation process [22]. If the fluidity of CPB is insufficient, it may not be evenly filled to the target stope and even lead to pipe-blocking accidents [23,24]. Therefore, understanding the rheological properties of FRCPB, especially the mechanism of fibers, is of great significance to optimizing the transportation process of FRCPB and thereby improving mining efficiency and quality.

The water film thickness (WFT) theory may be a practical and promising method to reveal the mechanism of fibers on the rheological properties of FRCPB [25–28]. After the water in the system fills the voids of the particles, the excess free water forms a water film on the particles' surface, which is an important factor in controlling the fluidity of the slurry [28]. WFT was originally proposed to evaluate the fluidity of cement paste, mortar, and concrete [29,30]. Compared with mortar or concrete, CPB has significantly higher water content and much lower binder content [31,32]. Qiu et al. [28,33] confirmed the applicability of WFT theory to traditional CPB. On this basis, Guo et al. [34] used WFT theory to study the fluidity of superfine-tailings cemented paste backfill and proposed the concept of floc film thickness. Additionally, WFT has proven critical to understanding the flow behavior of backfill materials containing hydrogen peroxide or biomass power plant ash [35]. In summary, WFT has relevant applications in the fluidity of backfill materials. However, to the authors' knowledge, there are currently few relevant studies on the use of WFT to explore the rheological properties of CPB-containing fibers.

Based on the above discussion, the originality of this study lies in introducing the concept of WFT to explore the mechanism of polypropylene fiber (PPF) on the rheological properties of CPB. Through dry and wet packing tests, the packing density of the tailings-binder-PPF (TBP) solid mixture system was obtained, and the WFT was calculated based on this. In addition, the rheological properties (yield stress and thixotropy, etc.) of CPB containing different PPF contents were measured. Finally, the yield stress and WFT of FRCPB were correlated, and the quantitative relationship between them was obtained.

2. Experimental Materials and Methods

2.1. Experimental Materials

The raw materials used in this study include tailings, cementitious materials, mixing water and fiber.

2.1.1. Tailings

The tailings used to prepare CPB come from the Aoniu iron ore mine in northeast China, and its specific gravity is 2.83. Figure 1a shows the particle size distribution of tailings obtained by the Mastersizer 2000. It can be seen from the figure that the fine content (<20 μm) of tailings is 25.01%, which can be regarded as coarse tailings [36]. The non-uniformity coefficient (*Cu*) and curvature coefficient (*Cc*) of tailings are 8.93 and 2.17, respectively, indicating a good particle gradation [22]. X-ray fluorescence (XRF) results show that the main chemical components of tailings are SiO_2 (53.99%), Fe_2O_3 (22.84%), Al_2O_3 (8.51%), CaO (6.38%) and MgO (5.38%). In addition, X-ray fluorescence (XRF) analysis shows that the main minerals of tailings are quartz, diopside, anorthite, hornblende, and magnetite (Figure 1b).

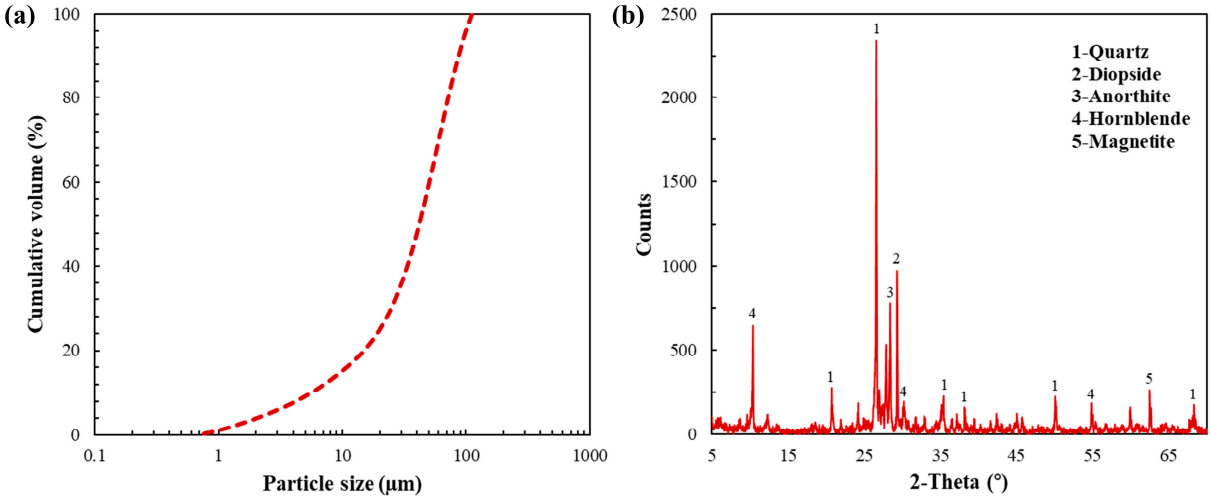

Figure 1. (**a**) Particle size distribution of tailings; (**b**) XRD results of tailings.

2.1.2. Cementitious Materials and Water

The cementitious materials are used to provide the strength required for the CPB sample [37]. Ordinary Portland cement, P·O 42.5, is used as a cementitious material. Its specific surface area and specific gravity are 5003 cm^2/g and 3.2, respectively. The main chemical components of cement are CaO (60.16%), SiO_2 (22.46%), Fe_2O_3 (5.86%), Al_2O_3 (4.65%), and MgO (2.32%). In addition, granulated blast furnace slag is used as a mineral admixture to replace part of the cement. The mass ratio of cement to slag is set to 3:2. The cement-to-slag ratio was chosen to optimize cost, enhance sustainability, and improve rheological properties by leveraging the synergistic effects between cement and blast furnace slag. Tap water is used as mixing water to homogenize the tailings, binder and fibers.

2.1.3. Fiber

The incorporation of fibers aims to enhance the toughness, flexural strength, and tensile properties of cement-based materials [38–40]. The fiber selected is polypropylene fiber (PPF), commonly used in the backfill field, and its density and Young's modulus are 0.91 g/cm^3 and 3.85 Gpa, respectively (Figure 2). The reason for choosing PPF is that PPF has excellent mechanical properties, chemical resistance, and compatibility with cementitious materials. PPFs are widely used in CPB to improve mechanical performance by mitigating shrinkage and cracking, as well as enhancing the post-yield strength and ductility of the backfill.

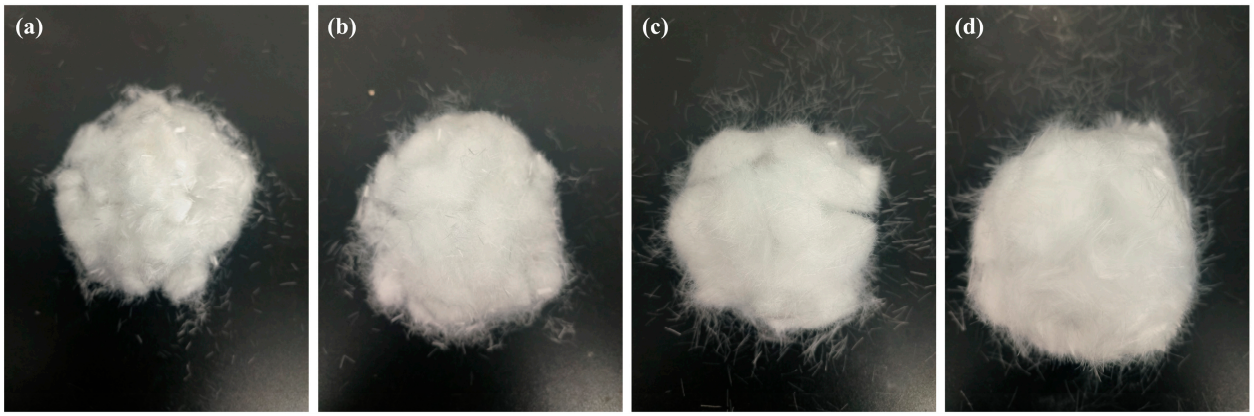

Figure 2. PPF selected for the experiment: (**a**) 3 mm; (**b**) 6 mm; (**c**) 9 mm; (**d**) 12 mm.

2.2. Experimental Methods

The CPB samples with different PPF contents (0%, 0.1%, 0.2%, 0.3%, and 0.4%) were prepared, and the fiber content was expressed as a volume percentage of solid dry material (tailings and binder). In addition, PPF lengths are 3, 6, 9, and 12 mm, respectively. Detailed mix proportions can be seen in Table 1. It should be noted that, except for the WFT test (68%, 69%, 70%, and 71%), the solid content and binder dosage of other CPB samples were fixed at 71% and 10%, respectively. The selection of the solid content was based on a balance between achieving adequate flowability and ensuring sufficient mechanical strength of CPB. The binder dosage was calculated based on the weight of the solid components, which include the tailings and any added mineral admixtures. The relatively high cement content was adopted to ensure sufficient early-age strength and durability of the CPB. The water added to the mixture was determined based on achieving the target solid content of 71%. After the preset material is prepared, the dry material is mixed evenly first, and then the required water is added to further stir for 3 min to ensure the uniform distribution of the fiber to the maximum extent. The preparation process of fresh FRCPB is shown in Figure 3.

Table 1. The mix proportions of the experimental FRCPB samples.

Solid Content/%	Binder Dosage/%	PPF Content/%	PPF Length/mm
71	10	0, 0.1, 0.2, 0.3, 0.4	3, 6, 9, 12

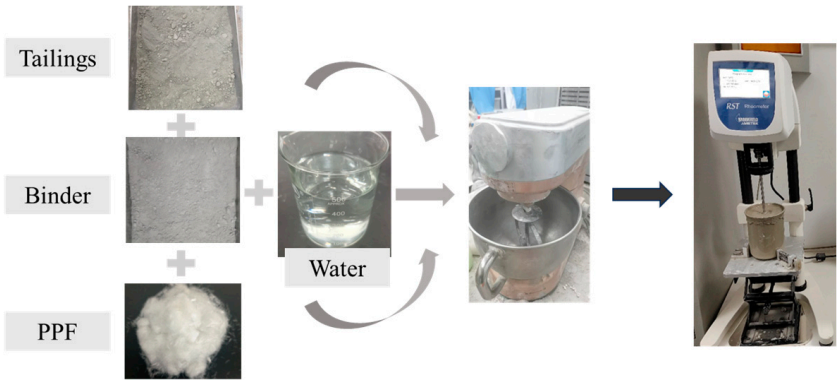

Figure 3. The preparation process of fresh FRCPB.

2.2.1. Determination of Packing Density

In this paper, the dry packing test and wet packing test were used to measure the packing density. The dry packing test was carried out in a water-free environment, and the specific steps are as follows: First, weigh the required tailings, binder, and PPF, then mix

the tailings and binder thoroughly for 2 min using a mixer, followed by the addition of PPF and further mixing for 2 min. Transfer the mixed dry materials into a measuring container and vibrate on a vibrating table for 1 min to minimize workmanship variation. Detailed experimental procedures for the dry packing test can be found in [41]. Finally, the packing density of the TBP system ($\varnothing_{dry}$) obtained by the dry packing test can be calculated using the following formula:

$$\varnothing_{dry} = \frac{\rho_{bulk}}{\rho_t\alpha_t + \rho_b\alpha_b + \rho_f\alpha_f} \quad (1)$$

where ρ_{bulk} is the bulk density of the sample in the container; ρ_t, ρ_b and ρ_f are the densities of tailings, binder, and PPF, respectively; α_t, α_b and α_f refer to the volume fraction of tailings, binder, and PPF in solid materials, respectively.

When measuring packing density using the wet packing test, the water content in the solid system is continuously increased, causing an initial increase in the solid concentration due to the formation of liquid bridges, followed by a decrease due to particle dispersion and an increase in slurry volume [42]. The highest solid concentration reached by the system is considered its packing density. In conducting a wet packing test, the water-to-solid (W/S) ratio is first set, and the required amounts of tailings, binder, and PPF are weighed. The tailings, binder, and water are thoroughly mixed for 2 min using a mixer, after which PPF is added and mixed for an additional 2 min. The resulting slurry is then transferred to a measuring container and vibrated for 1 min on a vibrating table. Finally, the packing density of the TBP system ($\varnothing_{wet}$) obtained by the wet packing test can be calculated using the following formula:

$$\varnothing_{wet} = \frac{\rho_{bulk}}{\rho_w\beta_w + \rho_t\alpha_t + \rho_c\alpha_c + \rho_f\alpha_f} \quad (2)$$

where ρ_w is the density of water, and β_w is the volumetric W/S ratio.

2.2.2. Determination of WFT

WFT was determined to study the mechanism of PPF on the rheological properties of CPB. According to the WFT theory [43], the water incorporated into the system can be divided into two parts: void-filling water and excess water, where the excess water forms a water film enveloping the surfaces of solid particles. After obtaining the packing density of the solid system, WFT can be expressed by the following equation:

$$WFT = \frac{w_0 - w_1}{A_s} \quad (3)$$

where w_0 and w_1 represent the total water volume ratio and void volume ratio, respectively, and $w_0 - w_1$ represents the excess water volume ratio. w_1 can be represented as $\frac{1-\varnothing}{\varnothing}$, where $\varnothing$ represents the packing density of a solid system. A_s is the total specific surface area of the solid material, and the specific calculation method can be found in [25].

2.2.3. Determination of Yield Stress and Thixotropy

The prepared FRCPB is transferred to the measuring cup of the rheometer, followed by rheological testing. It should be noted that the length of the fiber is fixed at 6 mm. The rheometer used is a Brookfield RSR-CC. The shear protocol used here (Figure 4a) is as follows: pre-shear at a rate of 100 s^{-1} for 60 s, followed by a rest period of 30 s. The pre-shear serves to homogenize the slurry and eliminate any residual structure, providing a consistent baseline before measuring the buildup of structure during the rest period. The rest step allows the system to recover and rebuild the internal structure, which is essential for assessing thixotropy. After resting, the shear rate increases linearly from 0 to 100 s^{-1} and then decreases linearly to 0 in 120 s. This shearing pattern mimics the conditions experienced in practical pumping and flow scenarios. The data obtained from

the descending segment are fitted using the Herschel–Bulkley (H–B) rheological model to determine the rheological parameters. The model is as follows:

$$\tau = \tau_0 + \mu\dot{\gamma}^n \quad (4)$$

where τ and τ_0 are shear stress and (dynamic) yield stress, respectively. μ is the consistency index, $\dot{\gamma}$ is the shear rate, and n is the H–B index indicating the degree of shear thinning or thickening.

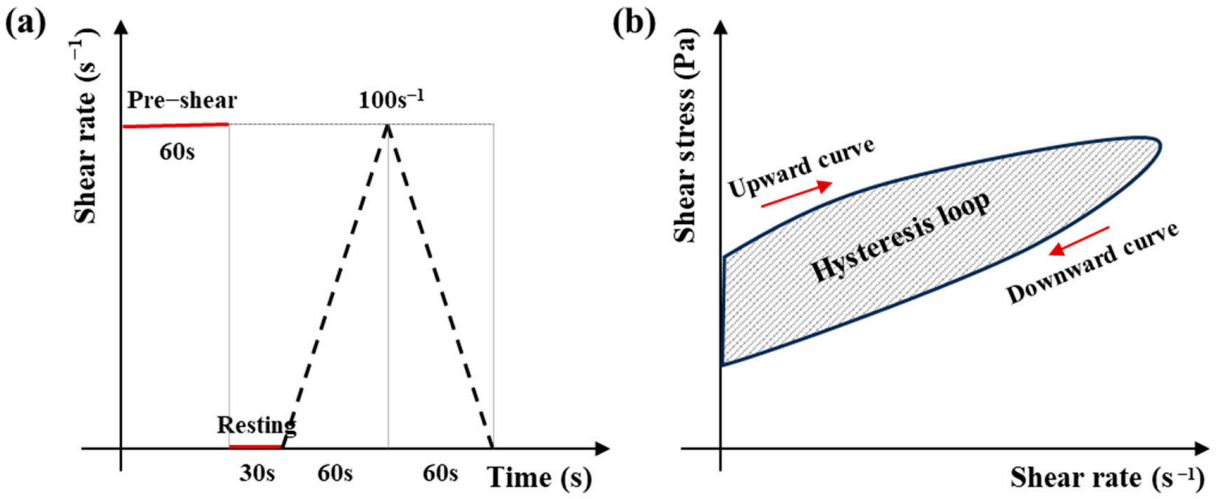

Figure 4. (**a**) Rheological protocol; (**b**) schematic diagram of the thixotropic hysteresis loop.

After obtaining the shear stress–shear rate curves through the above shear protocol, the area of the hysteresis loop formed by the upward and downward curves (Figure 4b) can be used to characterize the thixotropy of FRCPB. A larger area of the hysteresis loop indicates stronger thixotropy of the slurry, and vice versa [44].

3. Results and Discussions

3.1. Packing Density and WFT

3.1.1. Effect of Water Content on Solid Concentration

Figure 5 shows the variation in solid concentration with the W/S ratio in a solid mixture system containing 0.2% PPF (length = 6 mm) under dry and wet conditions. When the W/S ratio is zero, that is, there is no water in the system, and the solid mixture system is in a dry environment, the solid concentration at this time is equal to the packing density obtained by the dry packing test. With the increase in the W/S ratio, the solid concentration initially decreases and then gradually increases. The initial decrease in solid concentration, known as the "bulking effect", is caused by the formation of a water film on the particle surfaces that leads to an air interlock, pushing the solid particles apart [41]. However, after reaching a certain water content, the water films begin to merge, forming what are known as "liquid bridges" and the excess water starts to fill the voids, leading to an increase in solid concentration [34]. It can be also seen from the figure that after the solid concentration reaches a maximum value (0.675, packing density), it begins to decrease with the water content. This is because the excess water separates the particles, causing the particles to become dispersed and thus increasing the volume of FRCPB, ultimately leading to a decrease in the solid concentration. In addition, the evolution of void ratio corresponds to the result of packing density, exhibiting a pattern of increasing, then decreasing, and finally increasing. When the system reaches its maximum packing density, the void ratio is at its lowest, indicating that the system has achieved its maximum compactness at this point.

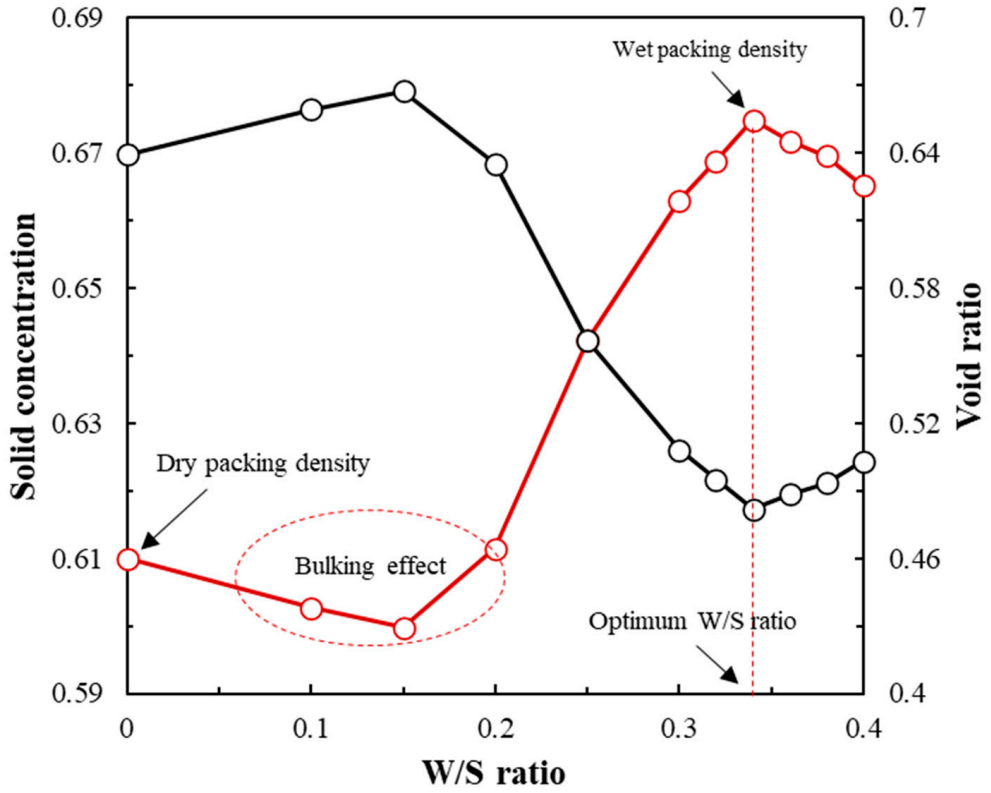

Figure 5. Solid concentration of CPB containing 0.2% PPF (fiber length = 6 mm).

3.1.2. Effect of PPF on Packing Density

The packing densities of the TBP system obtained from dry and wet packing tests are shown in Figure 6. It is evident that the packing densities obtained from the dry packing test range between 0.569 and 0.603, while those from the wet packing test range from 0.620 to 0.677. Therefore, the results from the wet packing test are higher than those from the dry packing test, indicating that water has a significant positive impact on the packing of the TBP system. The reason for this phenomenon may be that water can reduce the agglomeration of particles and fibers and lubricate them, resulting in a closer packing of particles and fibers, that is, a higher packing density [45]. In addition, in a wet environment, regardless of PPF length, the packing density of the system increases first with the fiber content and then decreases after reaching the maximum value. Therefore, similar to the filling effect of fine particles, there is an optimal PPF content that maximizes the packing density of the system [28]. This phenomenon can be explained as follows: when the PPF content is low, the fibers fill the voids between solid particles, which coincides with a decrease in void ratio, thus increasing the packing density. When the PPF content is high, some isolated fibers become trapped in the narrow gaps between solid particles, causing the particles to be wedged and separated, which increases the inter-particle spacing and thereby reduces the packing density. This phenomenon is known as the "wedge effect" [46]. On the other hand, it can also be observed from the figure that at a given fiber content, whether measured dry or wet packing test, the packing density slightly decreases with the increase in fiber length. This suggests that the length of PPF has a detrimental effect on the packing density of the TBP system. Therefore, although the fiber may bend and deform to fill or pass through the gap of particles due to the influence of slurry consistency, the wedge effect will increase if the fiber length increases, thus reducing the packing density [47].

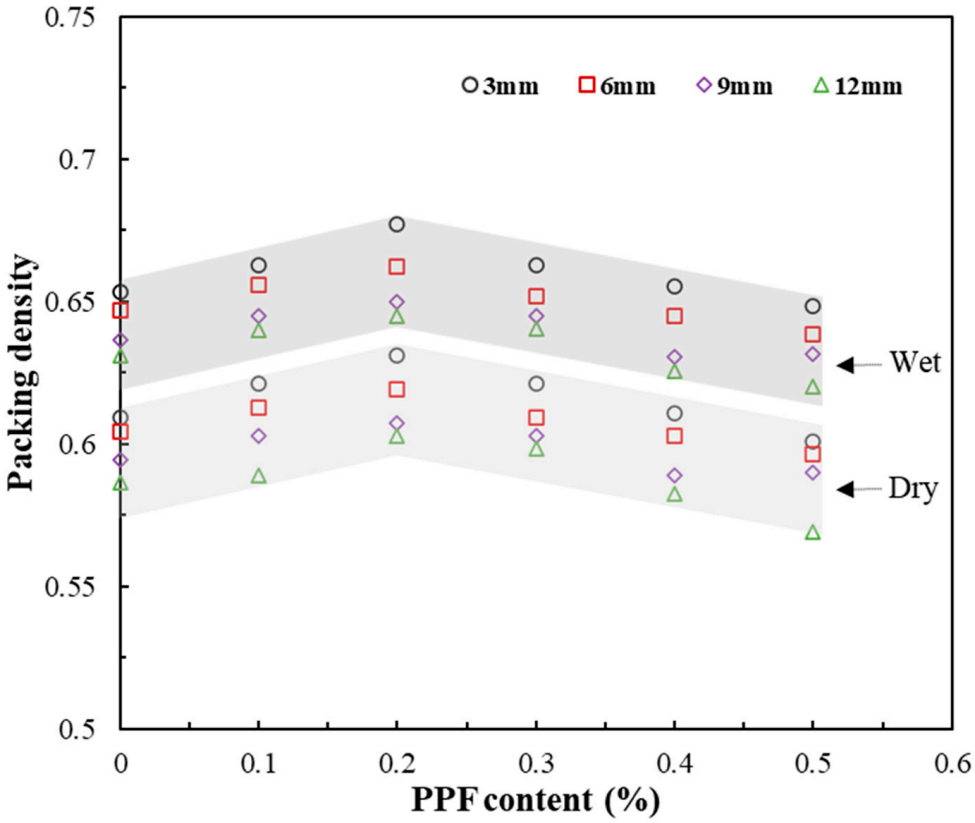

Figure 6. Packing densities of CPB containing fiber under wet and dry conditions.

Overall, the results obtained from the wet packing test seem to be more accurate than those from the dry packing test. In fact, in the absence of water, the forces acting between particles are primarily controlled by friction [48]. Therefore, due to higher resistance, it is difficult for the particles to rearrange and achieve close packing. In wet environments, however, the addition of water can provide lubrication and reduce friction between particles. This allows the particles to slide more smoothly and effectively into a more compact arrangement [28]. It should be noted that the wet environment is also more consistent with the actual situation of the particles in the slurry and the influence of some admixtures such as superplasticizer can be considered. Therefore, for TBP systems, the wet packing test is a more scientific approach to measuring packing density.

3.1.3. Effect of PPF on WFT

The variation of WFT in CPB under different PPF contents and solid contents is shown in Figure 7. For ease of comparison, the PPF length is fixed at 6 mm. It is evident from the figure that regardless of the PPF content, WFT decreases as the solid content increases, which is due to the reduction in the system's water content. For example, at a given PPF content (0.2%), when the solid content increases from 68% to 71%, the WFT decreases from 0.561 to 0.498 μm. In addition, it can be noted that when the solid content remains constant, WFT increases first and then decreases with the PPF content. This corresponds to the result of packing density. A greater packing density results in a lower void ratio, so when the solid content is equal, a higher amount of excess water is required to cover the solid surface to form a water film, leading to a greater WFT. It is also important to note that increasing the fiber content decreases the total specific surface area of the solids system, which leads to an increase in WFT. Therefore, WFT is the result of the coupling of packing density and specific surface area.

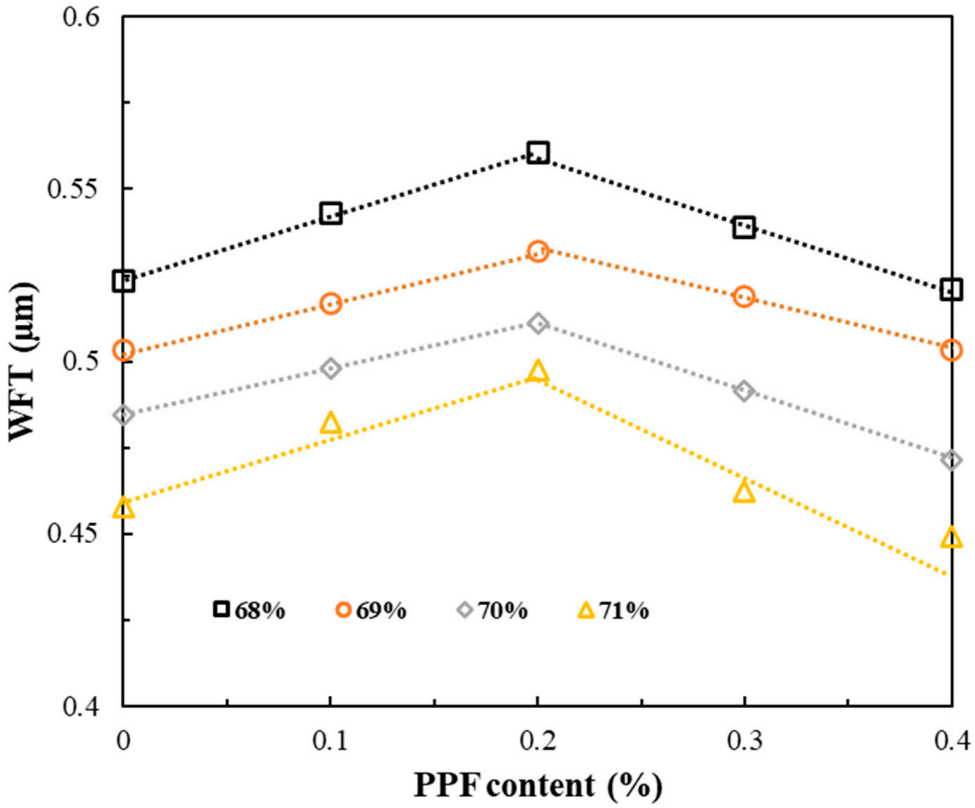

Figure 7. Effects of PPF content and solid content on WFT of CPB.

Compared to the WFT of mortar and cement paste, the WFT of FRCPB is significantly greater due to its lower solid content [49,50]. This is consistent with the results of traditional CPB [28]. Additionally, a negative WFT (i.e., the voids between solid particles are not completely filled with water) does not occur in FRCPB, which is also due to the high water content of CPB.

3.2. Rheological Properties

Figure 8a shows the typical rheological curves of fresh CPB at a fixed solid content (71%) and binder dosage (10%) with different PPF dosages (0, 0.1%, 0.2%, 0.3%, and 0.4%). Table 2 presents the fitting results of the H–B model. Firstly, the fitted correlation coefficients are all greater than 0.98, indicating that the H–B model can well describe the rheological behavior of FRCPB and demonstrate that fresh FRCPB is a non-Newtonian fluid with yield stress. In addition, all FRCPBs exhibit significant shear-thinning behavior, which is similar to the rheological behavior displayed by ordinary CPB under shear. Samples with higher PPF content show more pronounced shear-thinning behavior, manifested by a smaller H–B index (Table 2). The fresh slurries exhibit either shear-thinning or shear-thickening behavior under shear, depending on the aggregation and breakage kinetics of the flocs [51]. When the breakage caused by shear dominates, the slurry exhibits characteristics of shear-thinning and vice versa. Therefore, PPF, to a certain extent, makes the flocs in CPB more susceptible to disruption. This may be related to the orientation of the fibers in the slurry. Furthermore, the yield stresses for CPBs containing 0, 0.1%, 0.2%, 0.3%, and 0.4% PPF are 23.59, 18.83, 15.9, 23.28, and 30.85 Pa, respectively. This trend is consistent with the changes in packing density, indicating that packing density may be an important factor affecting the rheological properties of FRCPB. Since WFT is a comprehensive representation of packing density and solid content among other factors, it is necessary to further investigate the relationship between WFT and yield stress.

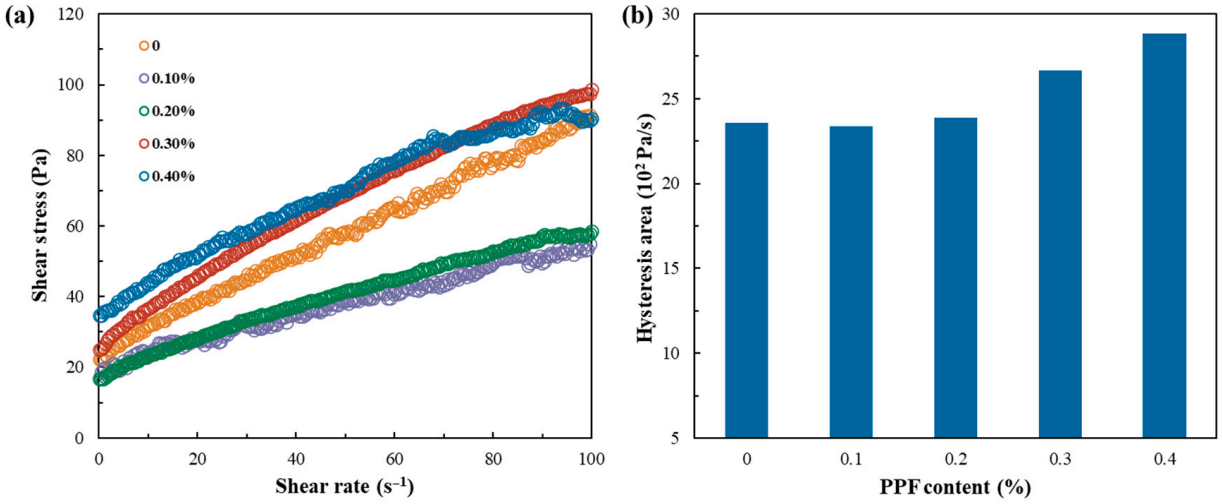

Figure 8. (**a**) Rheological curves of CPB with different PPF contents (0%, 0.10%, 0.20%, 0.30%, and 0.40%); (**b**) effect of PPF content on the hysteresis loop area of CPB.

Table 2. Fitting parameters of H–B model (τ_0: yield stress; μ: consistency index; n: H–B index).

PPF Content/ %	τ_0/ Pa	μ/ -	n/ -	R^2/ -
0	23.59	0.85	0.95	0.99
0.1	18.83	0.63	0.88	0.98
0.2	15.9	1.26	0.77	0.99
0.3	23.28	2.43	0.75	0.99
0.4	30.85	2.87	0.68	0.99

Figure 8b shows the variation of the hysteresis loop area of CPB with the amount of fiber added. It is apparent that when the fiber content is low (0%–0.2%), the hysteresis loop area remains relatively stable, around 2361 Pa/s. The area of the hysteresis loop represents the magnitude of thixotropy. Therefore, although the addition of a certain amount of fiber increases the system's packing density, it does not affect the thixotropy of CPB. Similar results were observed in Guo et al.'s study on the structural build-up of CPB containing RTPF [21]. If the fiber content is further increased, the hysteresis loop area begins to increase, indicating that fibers enhance the thixotropy of CPB. Therefore, low amounts of fiber do not significantly affect the macrostructure of CPB. However, when the fiber content reaches a certain level, fibers begin to form complex physical network structures within the slurry; this not only enhances the structural integrity and improves the viscosity, but also affects the dynamic shear process—these networks will partially destroy and quickly recover after stopping the shear, thus improving the thixotropy. It is important to note that the fiber content at the maximum packing density of the system precisely corresponds to the critical point where the thixotropy of FRCPB stabilizes and increases. This suggests that packing density may be an important factor affecting the thixotropy of FRCPB. On the other hand, thixotropy does not show a simple linear relationship with packing density. Thus, it can be inferred that in addition to packing density, there are other significant factors affecting the thixotropy of FRCPB, such as the interactions among fibers. This requires further exploration.

3.3. Discussion

The above results show that the optimal fiber content for achieving the best transport properties lies at 0.2%. At this fiber content, the CPB demonstrated sufficient viscosity to prevent segregation and bleeding while maintaining acceptable flowability for pipeline transport, i.e., low yield stress. In addition, it is also shown that WFT may be an important

factor affecting the yield stress of fresh FRCPB. Therefore, to further explore the mechanism of PPF on the yield stress of CPB, a relationship between WFT and yield stress has been established, as shown in Figure 9. It can be seen that, in general, the yield stress of FRCPB decreases with the increase in WFT. This is because when an external shear load is applied, particles adapt to the stress by sliding through the water film layer. The greater the WFT, the less direct contact between particles, thereby reducing friction and lowering the external stress required to initiate slurry flow [34]. In addition, a fitting analysis was carried out to quantify the relationship between WFT and the yield stress of fresh FRCPB. The fitting results show that there is a linear relationship between WFT and yield stress, with a correlation coefficient of 0.92. The *F*-test (95% level of confidence) was conducted to evaluate the significance of regression, and the results indicate a *p*-value of 1.35×10^{-7}, which is far less than 0.05, demonstrating the validity of the fitting equation. Therefore, it can be concluded that WFT is an important factor affecting the rheological properties of FRCPB. Qiu et al. also reached a similar conclusion when studying the fluidity of traditional fresh CPB [28]. The fitting equation can be used to predict the yield stress of FRCPB, which has a certain significance for the field application of FRCPB.

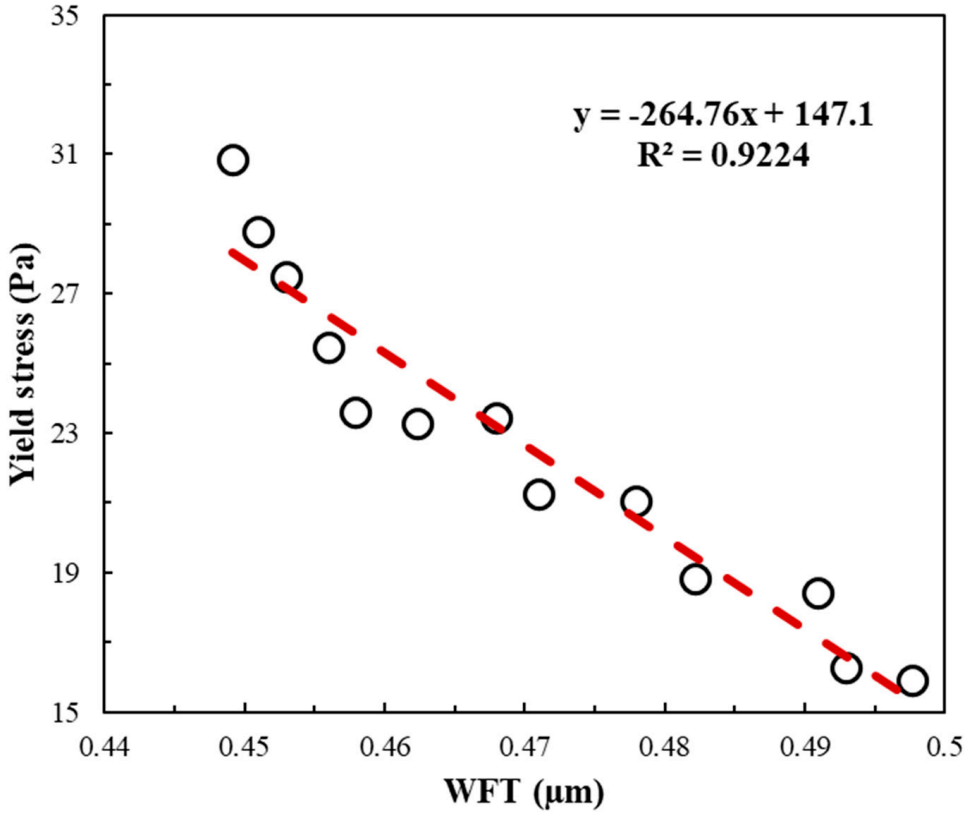

Figure 9. Relationship between WFT and yield stress of fresh FRCPB.

4. Conclusions

In this study, water film thickness (WFT) was introduced to explain the mechanism of polypropylene fibers (PPF) on the rheological properties of fresh CPB. Dry and wet packing tests were used to determine the packing density of solid systems with different fiber lengths (3 mm, 6 mm, 9 mm, and 12 mm) and fiber contents (0%, 0.1%, 0.2%, 0.3%, 0.4%, and 0.5%). On the basis of obtaining the packing density, the WFT was calculated. In addition, the rheological properties of fiber-reinforced cemented paste backfill (FRCPB), including yield stress and thixotropy, were measured. Based on the experimental results, the following conclusions can be drawn:

1. The packing density obtained by the wet packing test is greater than that obtained by the dry packing test. Compared with the dry packing test, the wet packing test is more suitable for measuring the packing density of the tailings-binder-PPF (TBP) system.
2. As the PPF content increases, the packing density of the TBP system first increases and then decreases. The increase in packing density is due to the filling effect of the fibers, while the decrease is attributed to the wedging effect. In addition, the PPF length has a slight adverse effect on the packing density.
3. The thixotropy of CPB exhibits a characteristic of stability followed by an increase with the addition of PPF. The critical PPF content for these two trends is 0.2%, at which point the system achieves its maximum packing density. Packing density is an important factor affecting the thixotropy of fresh FRCPB, but interactions among the fibers cannot be ignored.
4. The WFT tends to increase and then decrease with the PPF content. Moreover, there is a good linear relationship between WFT and the yield stress of fresh FRCPB. Therefore, WFT can be used to predict the yield stress of FRCPB.
5. The optimal PPF content was determined to be 0.2%, with a fiber length of 6 mm. This combination provides the best performance in terms of yield stress, thixotropy, and overall transport properties, making it suitable for use in CPB applications.

Author Contributions: Conceptualization, X.Z. and G.L.; methodology, X.Z. and H.W.; software, K.D., Q.H. and J.J.; validation, Y.L. (Yang Liu), B.L. and Y.M.; formal analysis, K.Z. and J.L.; investigation, H.Z.; resources, L.W.; data curation, J.W.; writing—original draft preparation, X.Z. and Y.L. (Yueming Lu); writing—review and editing, X.Z. and W.W.; visualization, D.L.; supervision, H.W.; project administration, H.W. All authors have read and agreed to the published version of the manuscript.

Funding: This research received no external funding.

Data Availability Statement: Data are contained within the article.

Conflicts of Interest: Xulin Zhao, Haijun Wang, Yang Liu, Yonggang Miao, Kunlei Zhu, Jianbo Liu are employees of BGRIMM Technology Group, Beijing 100160, China; Junchao Jin is employee of China Nonferrous Metal Mining (Group) Co., Ltd., Beijing 100029, China; Guanghua Luo, Kewei Dai, Qinghua Hu, Baowen Liu, Hai Zhang, Lianhe Wu, Jianming Wu, Yueming Lu, Wei Wang are employees of Ganfeng Lithium Group Co., Ltd., Xinyu 338000, China; Dingchao Lv is employee of Shanxi Zijin Mining Co., Ltd., Xinzhou 034302, China. The paper reflects the views of the scientists and not the company.

References

1. Solismaa, S.; Torppa, A.; Kuva, J.; Heikkilä, P.; Hyvönen, S.; Juntunen, P.; Benzaazoua, M.; Kauppila, T. Substitution of Cement with Granulated Blast Furnace Slag in Cemented Paste Backfill: Evaluation of Technical and Chemical Properties. *Minerals* **2021**, *11*, 1068. [CrossRef]
2. Bull, A.J.; Fall, M. Thermally Induced Changes in Metalloid Leachability of Cemented Paste Backfill That Contains Blast Furnace Slag. *Miner. Eng.* **2020**, *156*, 106520. [CrossRef]
3. Sagade, A.; Fall, M. Study of Fresh Properties of Cemented Paste Backfill Material with Ternary Cement Blends. *Constr. Build. Mater.* **2024**, *411*, 134287. [CrossRef]
4. Ouattara, D.; Mbonimpa, M.; Yahia, A.; Belem, T. Assessment of Rheological Parameters of High Density Cemented Paste Backfill Mixtures Incorporating Superplasticizers. *Constr. Build. Mater.* **2018**, *190*, 294–307. [CrossRef]
5. Al-Bakri, A.Y.; Ahmed, H.M.; Hefni, M.A. Experimental Investigation of Recycling Cement Kiln Dust (CKD) as a Co-Binder Material in Cemented Paste Backfill (CPB) Made with Copper Tailings. *Minerals* **2024**, *14*, 750. [CrossRef]
6. Dhers, S.; Guggenberger, R.; Freimut, D.; Fataei, S.; Schwesig, P.; Martic, Z. Impact of Admixtures on Environmental Footprint, Rheological and Mechanical Properties of LC3 Cemented Paste Backfill Systems. *Minerals* **2023**, *13*, 1552. [CrossRef]
7. Koc, E.; Cihangir, F. Ultrasonic and Microstructural Evaluation of Sulphide-Rich Tailings Cemented Paste Backfill Properties Containing Alkali-Activated Slag: Effect of Slag Fineness. *Minerals* **2023**, *13*, 1524. [CrossRef]
8. Cacciuttolo, C.; Marinovic, A. Experiences of Underground Mine Backfilling Using Mine Tailings Developed in the Andean Region of Peru: A Green Mining Solution to Reduce Socio-Environmental Impacts. *Sustainability* **2023**, *15*, 12912. [CrossRef]
9. Guo, Z.; Qiu, J.; Pel, L.; Zhao, Y.; Zhu, Q.; Kwek, J.W.; Zhang, L.; Jiang, H.; Yang, J.; Qu, Z. A Contribution to Understanding the Rheological Measurement, Yielding Mechanism and Structural Evolution of Fresh Cemented Paste Backfill. *Cem. Concr. Compos.* **2023**, *143*, 105221. [CrossRef]

10. Chakilam, S.; Cui, L. Effect of Polypropylene Fiber Content and Fiber Length on the Saturated Hydraulic Conductivity of Hydrating Cemented Paste Backfill. *Constr. Build. Mater.* **2020**, *262*, 120854. [CrossRef]
11. Libos, I.L.S.; Cui, L. Time-and Temperature-Dependence of Compressive and Tensile Behaviors of Polypropylene Fiber-Reinforced Cemented Paste Backfill. *Front. Struct. Civ. Eng.* **2021**, *15*, 1025–1037. [CrossRef]
12. Li, Z.; Shi, X.; Chen, X. Effect of Rice Straw on Tensile Properties of Tailings Cemented Paste Backfill. *Appl. Sci.* **2022**, *12*, 526. [CrossRef]
13. Chen, X.; Jiao, H.; Liu, J.; Yang, Y.; Chen, X.; Yang, L.; Zhang, W.; Yang, T. The Influence of Multi-Size Basalt Fiber on Cemented Paste Backfill Mechanical Properties and Meso-Structure Characteristics. *Minerals* **2023**, *13*, 1215. [CrossRef]
14. Xue, G.; Yilmaz, E.; Song, W.; Cao, S. Fiber Length Effect on Strength Properties of Polypropylene Fiber Reinforced Cemented Tailings Backfill Specimens with Different Sizes. *Constr. Build. Mater.* **2020**, *241*, 118113. [CrossRef]
15. Xue, G.; Yilmaz, E.; Song, W.; Yilmaz, E. Influence of Fiber Reinforcement on Mechanical Behavior and Microstructural Properties of Cemented Tailings Backfill. *Constr. Build. Mater.* **2019**, *213*, 275–285. [CrossRef]
16. Xue, G.; Yilmaz, E. Strength, Acoustic, and Fractal Behavior of Fiber Reinforced Cemented Tailings Backfill Subjected to Triaxial Compression Loads. *Constr. Build. Mater.* **2022**, *338*, 127667. [CrossRef]
17. Cao, S.; Yilmaz, E.; Song, W. Fiber Type Effect on Strength, Toughness and Microstructure of Early Age Cemented Tailings Backfill. *Constr. Build. Mater.* **2019**, *223*, 44–54. [CrossRef]
18. Chen, X.; Shi, X.; Zhou, J.; Chen, Q.; Li, E.; Du, X. Compressive Behavior and Microstructural Properties of Tailings Polypropylene Fibre-Reinforced Cemented Paste Backfill. *Constr. Build. Mater.* **2018**, *190*, 211–221. [CrossRef]
19. Sun, K.; Fall, M. Response Surface Methodology-Based Characterization and Optimization of Fibre Reinforced Cemented Tailings Backfill with Slag. *Int. J. Min. Reclam. Environ.* **2023**, *37*, 735–759. [CrossRef]
20. Cui, L.; McAdie, A. Experimental Study on Evolutive Fracture Behavior and Properties of Sulfate-Rich Fiber-Reinforced Cemented Paste Backfill under Pure Mode-I, Mode-II, and Mode-III Loadings. *Int. J. Rock Mech. Min. Sci.* **2023**, *169*, 105434. [CrossRef]
21. Guo, Z.; Qiu, J.; Kirichek, A.; Zhou, H.; Liu, C.; Yang, L. Recycling Waste Tyre Polymer for Production of Fibre Reinforced Cemented Tailings Backfill in Green Mining. *Sci. Total Environ.* **2024**, *908*, 168320. [CrossRef] [PubMed]
22. Haiqiang, J.; Fall, M.; Cui, L. Yield Stress of Cemented Paste Backfill in Sub-Zero Environments: Experimental Results. *Miner. Eng.* **2016**, *92*, 141–150. [CrossRef]
23. Carnogursky, E.A.; Fall, M.; Haruna, S. Rheology and Setting Time of Saline Cemented Paste Backfill. *Miner. Eng.* **2023**, *202*, 108258. [CrossRef]
24. Kou, Y.; Jiang, H.; Ren, L.; Yilmaz, E.; Li, Y. Rheological Properties of Cemented Paste Backfill with Alkali-Activated Slag. *Minerals* **2020**, *10*, 288. [CrossRef]
25. Li, L.G.; Chu, S.H.; Zeng, K.L.; Zhu, J.; Kwan, A.K.H. Roles of Water Film Thickness and Fibre Factor in Workability of Polypropylene Fibre Reinforced Mortar. *Cem. Concr. Compos.* **2018**, *93*, 196–204. [CrossRef]
26. Li, L.G.; Zhao, Z.W.; Zhu, J.; Kwan, A.K.H.; Zeng, K.L. Combined Effects of Water Film Thickness and Polypropylene Fibre Length on Fresh Properties of Mortar. *Constr. Build. Mater.* **2018**, *174*, 586–593. [CrossRef]
27. Li, L.G.; Zeng, K.L.; Ouyang, Y.; Kwan, A.K.H. Basalt Fibre-Reinforced Mortar: Rheology Modelling Based on Water Film Thickness and Fibre Content. *Constr. Build. Mater.* **2019**, *229*, 116857. [CrossRef]
28. Qiu, J.; Guo, Z.; Yang, L.; Jiang, H.; Zhao, Y. Effects of Packing Density and Water Film Thickness on the Fluidity Behaviour of Cemented Paste Backfill. *Powder Technol.* **2020**, *359*, 27–35. [CrossRef]
29. Fung, W.W.S.; Kwan, A.K.H. Role of Water Film Thickness in Rheology of CSF Mortar. *Cem. Concr. Compos.* **2010**, *32*, 255–264. [CrossRef]
30. Kwan, A.K.H.; Fung, W.W.S. Roles of Water Film Thickness and SP Dosage in Rheology and Cohesiveness of Mortar. *Cem. Concr. Compos.* **2012**, *34*, 121–130. [CrossRef]
31. Mater, Y.M.; Elansary, A.A.; Abdalla, H.A. Experimental and Numerical Investigation of Preloaded Recycled Concrete Beams Strengthened with CFRP. *World J. Eng.* **2024**. [CrossRef]
32. Rathore, S.S.; Meesala, C.R. Influence of Recycled Coarse Aggregate on Properties of Fly Ash and Slag-Based Geopolymer Concrete Cured under Oven and Ambient Temperature. *World J. Eng.* 2024; *ahead of print*.
33. Qiu, J.; Guo, Z.; Yang, L.; Jiang, H.; Zhao, Y. Effect of Tailings Fineness on Flow, Strength, Ultrasonic and Microstructure Characteristics of Cemented Paste Backfill. *Constr. Build. Mater.* **2020**, *263*, 120645. [CrossRef]
34. Guo, Z.; Qiu, J.; Jiang, H.; Xing, J.; Sun, X.; Ma, Z. Flowability of Ultrafine-Tailings Cemented Paste Backfill Incorporating Superplasticizer: Insight from Water Film Thickness Theory. *Powder Technol.* **2021**, *381*, 509–517. [CrossRef]
35. Qi, T.; Gao, X.; Feng, G.; Bai, J.; Wang, Z.; Chen, Q.; Wang, H.; Du, X. Effect of Biomass Power Plant Ash on Fresh Properties of Cemented Coal Gangue Backfill. *Constr. Build. Mater.* **2022**, *340*, 127853. [CrossRef]
36. Fall, M.; Benzaazoua, M.; Ouellet, S. Experimental Characterization of the Influence of Tailings Fineness and Density on the Quality of Cemented Paste Backfill. *Miner. Eng.* **2005**, *18*, 41–44. [CrossRef]
37. Benito, E.K.D.; Aragoncillo, A.M.M.; Pascua, F.A.A.; Juanites, J.M.; Eneria, M.A.; Zafra, R.G.; Madlangbayan, M.S. Durability Performance of Concrete Containing Recycled Coarse Aggregates Derived from Laboratory-Tested Specimens. *World J. Eng.* **2024**, *21*, 604–614. [CrossRef]
38. Margabandu, S.; Subramaniam, S.K. Influence of Fiber Stacking Sequences and Matrix Materials on Mechanical and Vibration Behavior of Jute/Carbon Hybrid Composites. *World J. Eng.* **2022**, *19*, 639–651. [CrossRef]

39. Poodipeddi, S.K.K.; Singampalli, A.; Rayala, L.S.M.; Ravula, S.S.N. Structural and Fatigue Analysis of Car Wheel Rims with Carbon Fibre Composites. *World J. Eng.* **2024**, *21*, 503–509. [CrossRef]
40. Kannan, H.; Prakash, K.S. Improving Structural Performance of Concrete Beams by U-Wrapped Basalt Fibre: A Retrofitting Approach. *World J. Eng.* **2024**, *21*, 267–274. [CrossRef]
41. Li, L.G.; Zhuo, H.X.; Zhu, J.; Kwan, A.K.H. Packing Density of Mortar Containing Polypropylene, Carbon or Basalt Fibres under Dry and Wet Conditions. *Powder Technol.* **2019**, *342*, 433–440. [CrossRef]
42. Wong, H.H.C.; Kwan, A.K.H. Packing Density of Cementitious Materials: Part 1-Measurement Using a Wet Packing Method. *Mater. Struct. Constr.* **2008**, *41*, 689–701. [CrossRef]
43. Li, L.G.; Kwan, A.K.H. Concrete Mix Design Based on Water Film Thickness and Paste Film Thickness. *Cem. Concr. Compos.* **2013**, *39*, 33–42. [CrossRef]
44. Jiang, H.; Fall, M.; Yilmaz, E.; Li, Y.; Yang, L. Effect of Mineral Admixtures on Flow Properties of Fresh Cemented Paste Backfill: Assessment of Time Dependency and Thixotropy. *Powder Technol.* **2020**, *372*, 258–266. [CrossRef]
45. Li, L.G.; Kwan, A.K.H. Packing Density of Concrete Mix under Dry and Wet Conditions. *Powder Technol.* **2014**, *253*, 514–521. [CrossRef]
46. Kwan, A.K.H.; Chan, K.W.; Wong, V. A 3-Parameter Particle Packing Model Incorporating the Wedging Effect. *Powder Technol.* **2013**, *237*, 172–179. [CrossRef]
47. Sultangaliyeva, F.; Carré, H.; La Borderie, C.; Zuo, W.; Keita, E.; Roussel, N. Influence of Flexible Fibers on the Yield Stress of Fresh Cement Pastes and Mortars. *Cem. Concr. Res.* **2020**, *138*, 106221. [CrossRef]
48. Kwan, A.K.H.; Fung, W.W.S. Packing Density Measurement and Modelling of Fine Aggregate and Mortar. *Cem. Concr. Compos.* **2009**, *31*, 349–357. [CrossRef]
49. Li, Y.; Chen, J.J.; Kwan, A.K.H. Roles of Water Film Thickness in Fresh and Hardened Properties of Mortar. *Adv. Cem. Res.* **2013**, *25*, 171–182. [CrossRef]
50. Kwan, A.K.H.; Wong, H.H.C. Effects of Packing Density, Excess Water and Solid Surface Area on Flowability of Cement Paste. *Adv. Cem. Res.* **2008**, *20*, 1–11. [CrossRef]
51. Ferron, R.D.; Shah, S.; Fuente, E.; Negro, C. Aggregation and Breakage Kinetics of Fresh Cement Paste. *Cem. Concr. Res.* **2013**, *50*, 1–10. [CrossRef]